

# The tumbling rotational state of 1I/'Oumuamua

Wesley C. Fraser<sup>1\*</sup>, Petr Pravec<sup>2</sup>, Alan Fitzsimmons<sup>1</sup>, Pedro Lacerda<sup>1</sup>, Michele T. Bannister<sup>1</sup>, Colin Snodgrass<sup>3</sup> and Igor Smolić<sup>4</sup>

**The discovery<sup>1</sup> of 1I/2017 U1 (1I/'Oumuamua) has provided the first glimpse of a planetesimal born in another planetary system. This interloper exhibits a variable colour within a range that is broadly consistent with local small bodies, such as the P- and D-type asteroids, Jupiter Trojans and dynamically excited Kuiper belt objects<sup>2–7</sup>. 1I/'Oumuamua appears unusually elongated in shape, with an axial ratio exceeding 5:1 (refs <sup>1,4,5,8</sup>). Rotation period estimates are inconsistent and varied, with reported values between 6.9 and 8.3 h (refs <sup>4–6,9</sup>). Here, we analyse all the available optical photometry data reported to date. No single rotation period can explain the exhibited brightness variations. Rather, 1I/'Oumuamua appears to be in an excited rotational state undergoing non-principal axis rotation, or tumbling. A satisfactory solution has apparent lightcurve frequencies of 0.135 and 0.126 h<sup>–1</sup> and implies a longest-to-shortest axis ratio of  $\geq 5:1$ , although the available data are insufficient to uniquely constrain the true frequencies and shape. Assuming a body that responds to non-principal axis rotation in a similar manner to Solar System asteroids and comets, the timescale to damp 1I/'Oumuamua's tumbling is at least one billion years. 1I/'Oumuamua was probably set tumbling within its parent planetary system and will remain tumbling well after it has left ours.**

Models of uniform rotation about a single spin axis moderately match 1I/'Oumuamua's observed brightness variations within a few nights<sup>1,4–6,8</sup>. These models are inadequate for the six-night span of collated photometry we consider here (see Methods), with no single rotation period adequately matching the full set of data (see Fig. 1). We find that models that consider linear increases or decreases in the spin period fare no better, producing equally inadequate matches. Similar conclusions have been made by investigators using a different dataset<sup>10</sup>.

A tumbling model<sup>11</sup> with non-principal axis rotation and free precession provides an adequate description of the photometry (see Fig. 1). The relative sparseness of the data prevents the determination of a unique set of frequencies; possible frequencies include 0.31, 0.26, 0.23, 0.16, 0.14, 0.12, 0.10 and 0.009 h<sup>–1</sup>. We have discounted values that are clearly commensurate with Earth's rotation, although it is possible that one may be real. It is clear that tumbling provides a reasonable explanation for the peculiar brightness variations of 1I/'Oumuamua, which cannot be explained by simple single-axis rotation. Unfortunately, given the finite set of observations due to its limited observability, it is unlikely that a unique solution will ever be determined for this object.

The most complete lightcurve previously published<sup>1</sup> has an amplitude of  $\sim 2.5$  magnitudes, from which a minimum axial ratio of  $a/c$  of  $\sim 10:1$  was suggested. Observing at non-zero phase angles  $\alpha$ , however, can enhance the apparent lightcurve amplitude by an

amount dependent on the optical surface scattering properties of the body. An enhancement of up to 0.018 magnitude/degree can occur for carbonaceous surfaces<sup>12</sup>, and an enhancement of  $\sim 0.03$  magnitude/degree can occur for S- and similar type asteroids<sup>13</sup>, due to the combined effects of optical scattering law, global shape and spin-pole inclination to the line of sight. As this early lightcurve was observed at  $\alpha \approx 20^\circ$ , and our dataset spans  $19 < \alpha < 24.5^\circ$ , the true conservative lower limit to the axial ratio from observations is  $a/c \gtrsim 5$ . We caution, however, that the optical surface scattering properties of interstellar objects are unknown at present.

Non-principal axis rotation of small asteroids with slow rotation periods is a well-known phenomena<sup>11</sup>. Tumbling can be brought about by collisions<sup>14</sup>, tidal torques in planetary close encounters<sup>15</sup>, cometary activity<sup>16</sup> or the Yarkovsky–O'Keefe–Radzievskii–Paddack effect<sup>17</sup>. It is eventually damped by internal friction and stress–strain forces removing the excess rotational energy above that of the basic rotational state around the body's principal axis with the largest moment of inertia. The timescale to return to principal axis rotation depends on the body's internal rigidity and anelasticity, and its initial rotation rate, density, size and shape<sup>18–20</sup>. As it is possible that 1I/'Oumuamua is either an icy comet-like body or more similar to organic-rich asteroids in the outer asteroid belt, we have estimated the timescale for it to return to principle axis rotation based on both possibilities (see Methods). We find that a rigid, organic-rich body with the observed apparent elongation and size<sup>1</sup> will take  $4 \times 10^{11}$  to  $4 \times 10^{12}$  years to stop tumbling. We note that recent theories<sup>20,21</sup> suggest that the timescales may be a factor of 7–9 shorter than estimates that use the classical formula<sup>18</sup>. For icy bodies, the damping timescale is one order of magnitude lower. A large fraction of Solar System asteroids smaller than  $\sim 200$  m are tumblers, even among the very fast rotators that have tensile strength; for example, 2000 WL107 (ref. <sup>11</sup>) and 2008 TC3 (ref. <sup>22</sup>). Their tumbling suggests that they have a higher rigidity than larger and more weakly structured asteroids, which results in long damping timescales. 1I/'Oumuamua may have a similarly prolonged damping timescale, which could be much longer than the age of the universe.

What induced the current tumbling of 1I/'Oumuamua? As the Yarkovsky–O'Keefe–Radzievskii–Paddack effect scales with incident stellar flux, and cometary activity only occurs within close proximity to a star, both should be negligible in interstellar space. The space density of interstellar objects similar in size or larger than 1I/'Oumuamua is estimated<sup>1,5,23,24</sup> as  $n \sim 0.1 \text{ au}^{-3}$  and they should have a typical local standard of rest encounter velocity of  $v \approx 25 \text{ km s}^{-1}$  (ref. <sup>25</sup>). The collisional lifetime for an interstellar object of effective radius  $R$  is  $\sim (nR^2v)^{-1} \sim 10^{19}$  years. With a lack of other mechanisms available, it is clear that the tumbling of 1I/'Oumuamua probably commenced in its home planetary system.

<sup>1</sup>Astrophysics Research Centre, Queen's University Belfast, Belfast, UK. <sup>2</sup>Astronomical Institute, Academy of Sciences of the Czech Republic, Ondřejov, Czech Republic. <sup>3</sup>Planetary and Space Sciences, School of Physical Sciences, The Open University, Milton Keynes, UK. <sup>4</sup>Scientific Computing Laboratory, Center for the Study of Complex Systems, Institute of Physics Belgrade, University of Belgrade, Belgrade, Serbia. \*e-mail: [wes.fraser@qub.ac.uk](mailto:wes.fraser@qub.ac.uk)

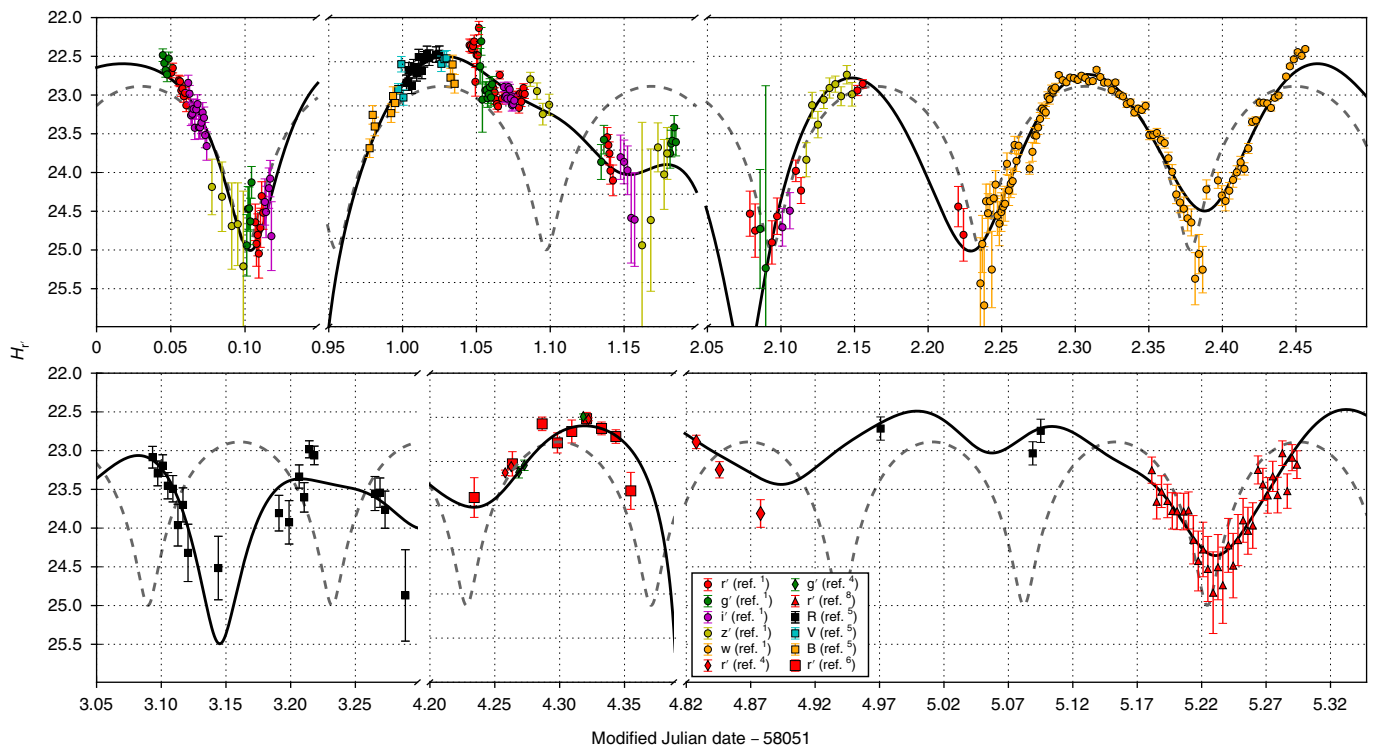


**Fig. 1 | The geometry-reduced and colour-corrected  $r'$ -band photometry,  $H_r$ , of 11/'Oumuamua cannot be well described by a model of simple rotation.** The dashed line depicts the best nominal period of 6.831h. The tumbling model lightcurve (solid line), however, is an adequate representation (see Methods for comments on the quality of the model fit to the lightcurve minima). Data sources and filters in which observations were acquired<sup>1,4–6,8</sup>, including some reanalysed data (see Methods), are indicated. Error bars represent  $1\sigma$  uncertainties in the photometry. Modified Julian date 58051 corresponds to a Gregorian date of 25 October 2017.

To estimate the shape of 11/'Oumuamua, a detailed physical model of its tumbling is needed. While lightcurve inversion<sup>21</sup> may be possible, such a technique makes a key assumption that the target possesses a uniform albedo, although, to date, 11/'Oumuamua's albedo remains unknown. Instead, we consider colour, noting that colour may not correlate with albedo. Within the six-day span available, colour variations have been detected for 11/'Oumuamua, suggesting a compositionally varied surface. Reported optical spectral slopes (see Methods) span  $0 \lesssim S' \lesssim 25\%/100$  nm. The veracity of the detected colour variations is demonstrated by the consistency of the different overlapping photometric datasets, after correction to  $r'$  using the reported colours from each dataset. Large colour variations cannot explain the unusual lightcurve behaviour of our multi-band dataset, as even when considering only observations made in  $r'$ , a single rotation period cannot be found. The observed colour variations appear to be correlated with the rotation of 11/'Oumuamua (see Fig. 2). Although only two red ( $S' \sim 25\%/100$  nm) measurements have been reported, both fall after the brightest phases of the lightcurve observed in the first two nights of the photometry sequence. All other colour measurements correspond to light-curve non-maxima and are neutral. The colour measurements imply that the body is largely a nearly neutral reflector with spectral slope  $S' \sim 5\%/100$  nm, and has a large red region.

11/'Oumuamua's colour variation is of a magnitude similar to the colour variations seen on some Kuiper belt objects<sup>26,27</sup>. It should be noted that the observed colours are roughly progressively more neutral with more recent observations (see Fig. 2b). It is tempting to attribute this to a trend of the surface of 11/'Oumuamua progressively evolving to a more neutral colour with time, as is observed in some Jupiter family comets and centaurs<sup>28</sup>. One of the red measurements, however, is bracketed by three neutral measurements taken over a span of a few hours on modified Julian date 58052 (see Fig. 2b), which is difficult to explain through surface colour

evolution. Rather, this colour sequence supports the idea of a spotted surface. Moreover, the idea of global colour evolution would require 11/'Oumuamua's transition from red to neutral to occur entirely within the six-day duration of the observations, 42–48 days after perihelion, in an unlikely serendipity of timing. It appears that 11/'Oumuamua's surface is inhomogeneously coloured.

## Methods

**Optical photometry.** Optical photometry data were compiled from refs<sup>1,4–6,8</sup>. Where available, observations were corrected to the  $r'$  filter in the Sloan Digital Sky Survey (SDSS) photometric system<sup>29</sup> using colours reported in those references or the temporally closest (g-r) colours<sup>1,4</sup> and assuming linear reflectance spectra through the optical range—an assumption that is consistent with reported spectra<sup>1–3</sup>. The published and corrected photometry data are tabulated in Supplementary Table 1.

Where temporal overlap between photometry datasets was available, consistency within the measurement uncertainties was checked. Only one inconsistency was found, occurring between the Gemini data from ref.<sup>4</sup> and the photometry data from ref.<sup>6</sup>. The data from ref.<sup>6</sup> were reanalysed using techniques similar to those made use of in ref.<sup>4</sup>. Specifically, median stacks of five images per stack were produced from the  $r'$  data. The data from ref.<sup>6</sup> were all acquired with the telescope tracking at near the rate of 11/'Oumuamua, although moderate tracking errors were apparent from deviations away from linearity in the stellar shapes. This necessitated the use of an elongated kernel for measuring star centroids. The on-image length and angle of those kernels was equal to the stellar trailing expected in each image. Stellar centroids were used for image alignment before stacking. Stacks were photometrically calibrated with in-image Sloan Digital Sky Survey stellar catalogue sources with (g-r) colour within 0.4 magnitudes of Solar. Photometry of the stars was measured using pill apertures, and photometry of 11/'Oumuamua was measured using a circular aperture with the Triled Image Photometry in Python package<sup>30</sup>. The aperture radii for stars and 11/'Oumuamua were 12 pixels, or roughly a full width at half maximum of 2, as any smaller resulted in divergent photometry, presumably as a result of the tracking errors. The resultant reanalysed photometry data were found to be fully consistent with the Gemini measurements of ref.<sup>4</sup> (see Fig. 1). Original photometry data, as well as colour- and geometry-corrected absolute magnitudes, are available in digital format.

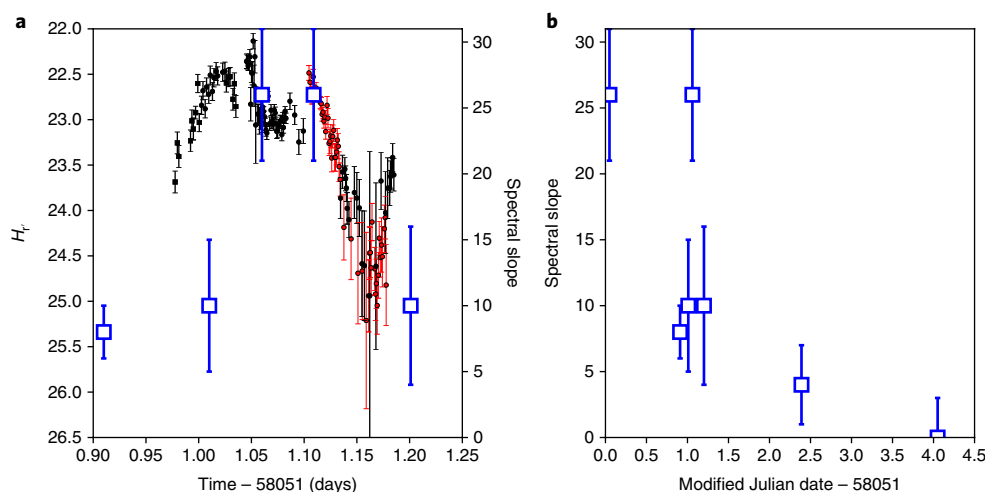


**Fig. 2 | Rotational colour variations.** **a**, Colour and geometry corrected photometry,  $H_r$ , of 1I/'Oumuamua from modified Julian date 58051 (red) shifted to match the lightcurve peak observed during modified Julian date 58052 (black). Colour measurements of 1I/'Oumuamua over this timespan are shown by the blue squares. **b**, All available colour measurements are presented as a function of time. Of the reported spectral slopes, only the reddest measurements correspond to peaks in the observed or modelled lightcurves, with the rest corresponding to lightcurve non-maxima. This argues for a body that is mainly a neutral reflector with a red region, although available colour measurements are insufficient to determine whether both of the long sides of 1I/'Oumuamua are red, or just one. Error bars represent  $1\sigma$  uncertainties on the photometry and colour measurements.

Spectral slopes (percent increase in reflectivity per 100 nm increase in wavelength normalized to 550 nm) were estimated from the reported colours<sup>1,4,5</sup> and spectra<sup>2,3</sup> assuming a linear spectrum through the optical range.

**Lightcurve modelling.** Simple rotation periods were searched for using phase dispersion minimization. The tumbling lightcurve was modelled following the technique of ref. <sup>11</sup>: a two-dimensional, second-order Fourier series was used to model the observed brightness variations, and satisfactory solutions were searched for in the two-dimensional frequency space. A number of possible combinations of frequencies were found to fit the lightcurve data, one of which provided a plausible fit and is presented in Fig. 1. Note, however, that due to the limited coverage of the lightcurve with the available data (missing observations from the longitudes of Asia/Australia in particular), the solution is not 'anchored' at uncovered times between the observational runs, allowing the fitted model to possibly under- or overestimate the brightness variation at those times. Without additional data breaking the commensurability of the observations with Earth's rotation, this problem cannot be solved. With the limited data, no Fourier series of an order higher than two could be used. While the second-order Fourier series describes the lightcurve data well at most rotational phases, some lightcurve minima are not accurately modelled, with the fit either under- or overestimating the depth. Additional data might enable the use of a third-order Fourier series, which would improve the model fit to the lightcurve minima.

**Damping timescales.** To estimate the damping timescales  $\tau_D$ , we used the formulation used previously in a study of small Solar system bodies<sup>18</sup>:

$$\tau_D \approx \frac{\mu Q}{\rho K_3^2 R^2 \omega^3}$$

where  $\mu$  is the rigidity of the object,  $Q$  is the anelasticity or damping constant,  $\rho$  is the bulk density and  $\omega$  is the angular velocity of rotation. For 1I/'Oumuamua, we take  $\omega = 2.36 \times 10^{-4} \text{ s}^{-1}$  from our analysis.  $K_3$  is a scaling coefficient that depends on the oblateness of the body  $p = (a - b)/a$ , where  $a$  and  $b$  are the semi-major and semi-minor axes of the body, respectively;  $K_3 \approx 0.1p^2$ . The lightcurve of ref. <sup>1</sup>, along with an assumed geometric albedo of 0.04, implies projected radii  $200 \times 20 \text{ m}$  ignoring amplitude-phase angle effects (see main text); hence, we use this to estimate a maximum oblateness of  $p \approx 0.9$  and  $K_3 \approx 0.08$ .

For an icy (or initially icy) comet-like body, we assume  $\rho \approx 1,000 \text{ kg m}^{-3}$ . The internal rigidity is unknown but we assume that  $\mu \approx 4 \times 10^9 \text{ N m}^{-2}$ , as was previously assumed for small bodies with weak strength<sup>31</sup>. The mean radius is given by  $R \approx \sqrt{ab} \approx 60 \text{ m}$ . A range of viable values of  $100 \leq Q \leq 1,000$  in turn implies  $4 \times 10^{10} \leq \tau_D \leq 4 \times 10^{11} \text{ years}$ . However, it is possible that 1I/'Oumuamua is instead a rocky object similar to C-type asteroids, such as those found predominantly in the outer main belt. In this case, we can assume  $\rho \approx 2,000 \text{ kg m}^{-3}$  and a rigidity that is a factor of 10 higher. At the same time, the geometric albedo could be higher at  $\approx 0.08$ , implying a corresponding reduction in  $R$ . This then predicts  $4 \times 10^{11} \leq \tau_D \leq 4 \times 10^{12} \text{ years}$ .

**Data availability.** All photometry data used in this manuscript are tabulated in Supplementary Table 1.

Received: 30 November 2017; Accepted: 23 January 2018;  
Published online: 09 February 2018

## References

- Meech, K. J., Weryk, R. & Micheli, M. A brief visit from a red and extremely elongated interstellar asteroid. *Nature* **552**, 378–381 (2017).
- Ye, Q.-Z., Zhang, Q., Kelley, M. S. P. & Brown, P. G. 1I/2017 U1 ('Oumuamua) is hot: imaging, spectroscopy, and search of meteor activity. *Astrophys. J. Lett.* **851**, L5 (2017).
- Fitzsimmons, A. et al. Spectroscopy and thermal modelling of the first interstellar object 1I/2017 U1 'Oumuamua. *Nat. Astron.* <https://doi.org/10.1038/s41550-017-0361-4> (2018).
- Bannister, M. T. et al. Col-OSSOS: colors of the interstellar planetesimal 1I/'Oumuamua. *Astrophys. J. Lett.* **851**, L38 (2017).
- Jewitt, D. et al. Interstellar Interloper 1I/2017 U1: observations from the NOT and WIYN telescopes. *Astrophys. J. Lett.* **850**, L36 (2017).
- Bolin, B. T. et al. APO time-resolved color photometry of highly elongated interstellar object 1I/'Oumuamua. *Astrophys. J. Lett.* **852**, L2 (2018).
- Masiero, J. Palomar optical spectrum of hyperbolic near-earth object A/2017 U1. Preprint at <https://arxiv.org/abs/1710.09977> (2017).
- Knight, M. M. et al. On the rotation period and shape of the hyperbolic asteroid 1I/'Oumuamua (2017 U1) from its lightcurve. *Astrophys. J. Lett.* **851**, L31 (2017).
- Feng, F. & Jones, H. R. A. 'Oumuamua as a messenger from the Local Association. *Astrophys. J. Lett.* **852**, L27 (2018).
- Drahus, M. et al. Tumbling motion of 1I/'Oumuamua reveals body's violent past. Preprint at <https://arxiv.org/abs/1712.00437> (2017).
- Pravec, P. et al. Tumbling asteroids. *Icarus* **173**, 108–131 (2005).
- Gutiérrez, P. J., Davidsson, B. J. R., Ortiz, J. L., Rodrigo, R. & Vidal-Núñez, M. J. Comments on the amplitude-phase relationship of asteroid lightcurves. Effects of topography, surface scattering properties, and obliquity. *Astron. Astrophys.* **454**, 367–377 (2006).
- Zappala, V., Cellino, A., Barucci, A. M., Fulchignoni, M. & Lupishko, D. F. An analysis of the amplitude-phase relationship among asteroids. *Astron. Astrophys.* **231**, 548–560 (1990).
- Henych, T. & Pravec, P. Asteroid rotation excitation by subcatastrophic impacts. *Mon. Not. R. Astron. Soc.* **432**, 1623–1631 (2013).
- Scheeres, D. J., Ostro, S. J., Werner, R. A., Asphaug, E. & Hudson, R. S. Effects of gravitational interactions on asteroid spin states. *Icarus* **147**, 106–118 (2000).
- Samarasinha, N. H. & Mueller, B. E. A. Relating changes in cometary rotation to activity: current status and applications to Comet C/2012 S1 (ISON). *Astrophys. J. Lett.* **775**, L10 (2013).

17. Vokrouhlický, D., Breiter, S., Nesvorný, D. & Bottke, W. F. Generalized YORP evolution: onset of tumbling and new asymptotic states. *Icarus* **191**, 636–650 (2007).
18. Burns, J. A. & Safronov, V. S. Asteroid nutation angles. *Mon. Not. R. Astron. Soc.* **165**, 403 (1973).
19. Sharma, I., Burns, J. A. & Hui, C.-Y. Nutational damping times in solids of revolution. *Mon. Not. R. Astron. Soc.* **359**, 79–92 (2005).
20. Breiter, S., Rožek, A. & Vokrouhlický, D. Stress field and spin axis relaxation for inelastic triaxial ellipsoids. *Mon. Not. R. Astron. Soc.* **427**, 755–769 (2012).
21. Pravec, P. et al. The tumbling spin state of (99942) Apophis. *Icarus* **233**, 48–60 (2014).
22. Scheirich, P. et al. The shape and rotation of asteroid 2008 TC<sub>3</sub>. *Meteorit. Planet. Sci.* **45**, 1804–1811 (2010).
23. Engelhardt, T. et al. An observational upper limit on the interstellar number density of asteroids and comets. *Astron. J.* **153**, 133 (2017).
24. Trilling, D. E. et al. Implications for planetary system formation from interstellar object 1I/2017 U1 ('Oumuamua). *Astrophys. J. Lett.* **850**, L38 (2017).
25. Grav, T. et al. The Pan-STARRS synthetic solar system model: a tool for testing and efficiency determination of the moving object processing system. *Publ. Astron. Soc. Pac.* **123**, 423–447 (2011).
26. Lacerda, P., Jewitt, D. & Peixinho, N. High-precision photometry of Extreme KBO 2003 EL<sub>61</sub>. *Astron. J.* **135**, 1749–1756 (2008).
27. Fraser, W. C., Brown, M. E. & Glass, F. The Hubble Wide Field Camera 3 Test of Surfaces in the Outer Solar System: spectral variation on Kuiper belt objects. *Astrophys. J.* **804**, 31 (2015).
28. Jewitt, D. Color systematics of comets and related bodies. *Astron. J.* **150**, 201 (2015).
29. Fukugita, M. et al. The Sloan Digital Sky Survey photometric system. *Astron. J.* **111**, 1748 (1996).

30. Fraser, W. et al. TRIPPy: Triled Image Photometry in Python. *Astron. J.* **151**, 158 (2016).
31. Harris, A. W. Tumbling asteroids. *Icarus* **107**, 209 (1994).

## Acknowledgements

W.C.F., A.F., M.T.B. and P.L. acknowledge support from Science and Technology Facilities Council grant ST/P0003094/1. M.T.B. also acknowledges support from Science and Technology Facilities Council grant ST/L000709/1. The work by P.P. was supported by the Grant Agency of the Czech Republic (grant 17-00774S). C.S. is supported by a Science and Technology Facilities Council Ernest Rutherford Fellowship and grant ST/L004569/1.

## Author contributions

W.C.F. compiled the common filter dataset, re-reduced observations where necessary and led the analysis and writing of the manuscript. P.P., P. L. and I.S. performed the lightcurve modelling and assisted with writing. A.F. calculated damping timescale estimates and assisted with writing the paper. M.T.B. and C.S. assisted with interpretation of the lightcurve results and writing the paper.

## Competing interests

The authors declare no competing financial interests.

## Additional information

**Supplementary information** accompanies this paper at <https://doi.org/10.1038/s41550-018-0398-z>.

**Reprints and permissions information** is available at [www.nature.com/reprints](http://www.nature.com/reprints).

**Correspondence and requests for materials** should be addressed to W.C.F.

**Publisher's note:** Springer Nature remains neutral with regard to jurisdictional claims in published maps and institutional affiliations.